

## PRINCIPLES OF CARRIER-SELECTIVE CONTACTS BASED ON INDUCED JUNCTIONS

Martin Bivour<sup>1</sup>, Christoph Messmer<sup>1</sup>, Lisa Neusel<sup>1</sup>, Florian Zähringer<sup>1</sup>, Jonas Schön<sup>1</sup>,  
Stefan W. Glunz<sup>1,2</sup>, Martin Hermle<sup>1</sup>,

<sup>1</sup>Fraunhofer Institute for Solar Energy Systems (ISE), Heidenhofstrasse 2, 79110 Freiburg, Germany

<sup>2</sup>Department of Sustainable Systems Engineering (INATECH), Albert-Ludwigs University Freiburg,  
Georges-Köhler-Allee 103, 79110 Freiburg, Germany

**ABSTRACT:** The applicability of different high (low) work function thin films for the formation of alternative hole (electron) selective contacts is currently (re-) explored for silicon solar cells. To provide some insight into contact schemes based on induced junctions their operation principles, important design parameters and losses are reviewed experimentally and with the help of numerical device simulations. Simulations with Sentaurus TCAD are used to address the importance of the work function and an efficient tunneling transport. It is highlighted that “non-selective” contacts will not obey the standard diode theory. This calls for an adapted loss analysis and one approach for this is presented for different hole contacts prepared by evaporation, sputtering, atomic layer deposition and PECVD. The results show that the “classical” electrical losses of selective contacts, like recombination and ohmic transport which are well quantified by  $J_0$  and the ohmic contact resistance, are not sufficient for the evaluation of “non-selective” contacts.

Keywords: Heterojunction, Inversion-layer, a-Si, Simulation, Fundamentals

### 1 INTRODUCTION

Passivating and carrier selective contacts [1] have the potential to overcome some of the intrinsic efficiency limitations of the established homojunction contact schemes. For the latter, doping of the silicon absorber surface is applied to obtain carrier selective device regions below the unpassivated metal electrodes. The high recombination in this regions results in high  $J_0$  and therefore moderate voltage at MPP and open-circuit conditions. Both, passivating and non-passivation carrier selective contacts typically obey the diode model described by the Shockley equations

$$J = J_{gen} - J_0 \{ \exp[qV / (n k_B T)] - 1 \} \quad (1)$$

One important assumption for this is that the voltage ( $V$ ) corresponds to the external voltage ( $V_{external}$ ) and that this external voltage matches the quasi-Fermi level splitting within the absorber at the edge of the contact (depletion) region. The latter voltage can be expressed by the implied voltage ( $V_{implied}$ ). This assumption ( $V_{external} = V_{implied}$ ) is typically fulfilled when the gradient in the majority carrier quasi-Fermi level in the contact region is negligible. This means that low-injection conditions in the contact region during operation must be maintained [2], i.e. that the majority carrier density remains well above the minority carrier density ( $n_{maj} \gg n_{min}$ ). Or, in a more general expression, that the conductivity of majority carriers remains well above those of the minority carriers ( $\sigma_{maj} = q \mu_{maj} n_{maj} \gg \sigma_{min} = q \mu_{min} n_{min}$ ) [3]. Basically, we define contacts to be “selective” for which  $V_{external} = V_{implied}$  and hence the validity of the diode equation is fulfilled. Accordingly, we define contacts to be “non-selective” when having a significant voltage loss in the contact region during operation leading to  $V_{external} < V_{implied}$ .

Similar to classical homojunctions, for TOPCon [4] and poly-Si [5] related contacts obtaining carrier selectivity is typically not the main design constraint. This is explained by the high doping efficiency of the partly crystalline silicon thin films and the c-Si wafer surface. It ensures that the majority carrier density in the contact region during equilibrium ( $n_{maj,0}$ ) is already much higher than the excess carrier density that will be added during operation ( $\Delta n = \Delta p$ ). Accordingly,

$$n_{maj} = n_{maj,0} + \Delta p \gg n_{min} = n_{min,0} + \Delta n$$

with  $\Delta n \gg n_{min,0}$ , is typically fulfilled. For TOPCon and poly-Si related contacts, an intermediate passivating dielectric buffer ( $SiO_x$ ) ensures that those contacts are not only selective but also passivating. Accordingly,  $J_0$  is low and the device characteristic and the limiting losses are well described by the diode equation.

The application of different high (low) work function thin films for the formation of passivating and hole (electron) selective contacts is another currently explored approach for silicon solar cells. So far, most promising candidates are transition metal oxide based heterojunctions leading to efficiencies of about 22 % [6], [7]. However, other materials are also under investigation [8]. Work in this field can be understood as a renaissance of the induced silicon junctions from the 1970’s [9] (e.g. metal-insulator-semiconductor) by taking advantage of (i) novel or better studied high (low) work function contact materials mainly adapted from organic electronics [10] and (ii) improvements of the passivating intermediate buffer layers (a-Si:H, ultrathin dielectrics). However, knowledge regarding relevant junction and material properties and their engineering, stability issues and the integration of those high (low) work function contact materials in the c-Si solar cell device architectures is still in its infancy. Basically, engineering towards sufficient selectivity seems to be of more importance compared to devices featuring n- and p-type doped carrier selective silicon regions.

Within this work the operation principles, important design parameters and losses of contact schemes based on induced junctions are reviewed experimentally and with the help of numerical device simulations. Simulations with Sentaurus TCAD are used to address the importance of the induced c-Si dark band bending, the voltage loss in the contact region, the band line-up and an efficient tunneling transport. Hole contacts prepared by evaporation, sputtering, atomic layer deposition and PECVD are screened and results for simple solar cells with  $MoO_x$ ,  $V_2O_x$  and a-Si:H(p) hole contacts are presented.

### 2 SIMULATION RESULTS

2.1 Work function and showcase for selective and non-selective contacts.

The importance of a high work function (WF) for a

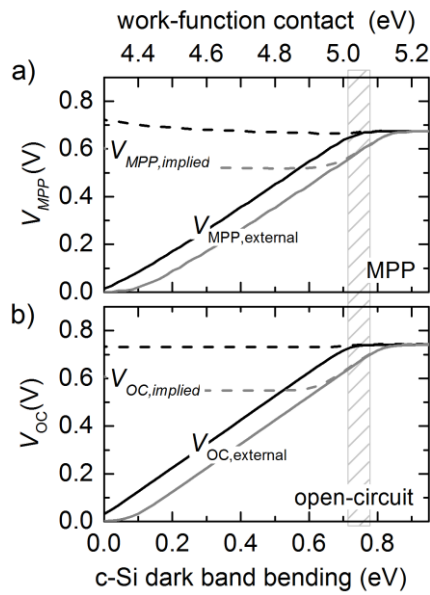


**Figure 1:** Simulated influence of work function and chemical c-Si passivation on the external and implied voltage for a) MPP and b) open-circuit conditions. For the grey lines poor chemical passivation is assumed ( $S_0=1000$  cm/s), for black lines  $S_0=10$  cm/s. The shaded region shows the transition between selective and non-selective contacts.

hole selective contact is motivated by simulating a n-type absorber with ideal electron contact and a metal / c-Si hole contact. Variables are the work function of a metal which is changed from extremely low values close to the c-Si work function (4.3 eV) to high values close above the c-Si valence band energy (5.17 eV). At the interface either excellent or poor chemical surface passivation is assumed.

The dashed lines in Figure 1 show that the implied voltage ( $V_{implied}$ ) is higher for the better chemical passivation (black line) for both MPP and open-circuit condition (except for very high WF). This reflects the higher density of excess holes and electrons in the absorber. The  $V_{implied}$  provides the upper limit of the extractable voltage. The external voltage approaches this value for a high WF and induced c-Si band bending ( $V_{bb}$ ) of above 5.0 eV and 0.7 eV, respectively. For lower values, power losses occur since the hole quasi-Fermi level in the hole contact region cannot be maintained. The corresponding gradient in the hole quasi-Fermi level represents the difference between the external voltage and implied voltage ( $\Delta V = V_{implied} - V_{external}$ ). Accordingly, when analyzing only the external voltage the upper limit of the extractable voltage provided by the passivation of the contact is underestimated by its insufficient selectivity. Therefore, a sufficient high equilibrium band bending and inversion of the c-Si surface is needed to build a hole selective contact ( $V_{external} \approx V_{implied}$ ). Good chemical passivation ensures that the voltage is on a high level.

Figure 2 explains why a work function above  $\sim 5.0$  eV is needed for a hole selective contact and negligible  $\Delta V$ . The blue line in Figure 2a shows how the equilibrium  $p/n$  ratio in the contact region is increased with increasing work function and induced c-Si band bending. During operation (MPP [orange], open-circuit [black]) this asymmetry is reduced by the increasing density of excess

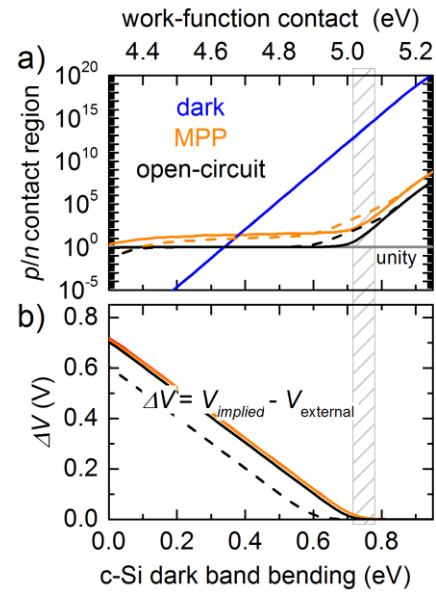


**Figure 2:** a) Simulated influence of work function on the ratio of hole and electron density at the metal / c-Si interface for equilibrium, MPP and open-circuit conditions. b) Corresponding difference between external and implied voltage. Solid lines show results for excellent and dashed lines for poor chemical passivation.

electrons and when  $p/n$  approaches unity (grey line)  $\Delta V$  becomes significant since  $n_{maj} \gg n_{min}$  and  $\sigma_{maj} \gg \sigma_{min}$  are not fulfilled anymore.

## 2.2 Transition metal oxide based silicon heterojunctions. Beyond the importance of the work function.

Figure 3 shows a possible band diagram featuring an inverted c-Si surface, an a-Si:H(i) passivation layer, a high band gap and high work function transition metal oxide (TMO) and a TCO electrode. While the importance of a high hole density for the c-Si part of the junction has been motivated before, the sketched band alignment suggests that for an efficient hole extraction from the c-Si towards the TCO an efficient tunneling transport should be involved as well. To derive some basic design rules

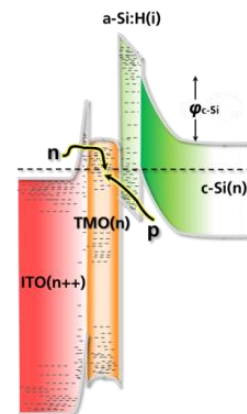


**Figure 3:** Sketched band diagram of a transition metal oxide based silicon heterojunction. An efficient hole transport via band-to-band tunneling is not possible since the conduction band energy of the TMO is below the valence band energy of the a-Si:H. Hence, the arrows indicate the need for trap assisted tunneling via the TMO.

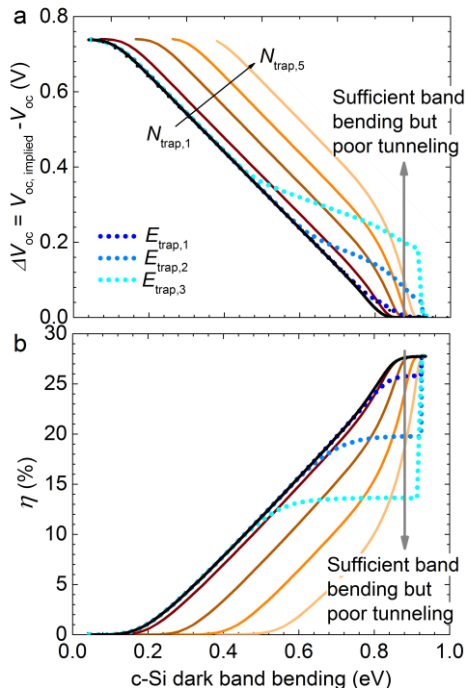


**Figure 4:** Simulated influence of work function and traps in the TMO on a) selectivity and b) efficiency of a contact similar to Figure 3.

and for better insight we performed more advanced numerical device simulations [11]. Figure 4 reviews some findings on the importance of an efficient tunneling via traps in the TMO. The latter is assumed to be essential for the case that the actual band alignment does not allow for band-to-band tunneling from the valance band of the a-Si:H(i) into the conduction band of the TMO. The black line in Figure 4 shows the case where trap assisted tunneling (TAT) is efficient.  $\Delta V$  and the efficiency are mainly limited by the induced c-Si band bending. Assuming a sufficient high band bending ( $> 0.8$  eV, grey arrows) it can be seen that for a reduction of the trap density ( $N_{\text{trap}1}$  [black]  $\rightarrow$   $N_{\text{trap}5}$  [orange]) the efficiency decreases due to an increased  $\Delta V$ . Another important parameter is the energetic position of the traps in the TMO. If the traps within the TMO are not energetically located close to the valance band of the buffer ( $E_{\text{trap}1}$  [blue]  $\rightarrow$   $E_{\text{trap}3}$  [cyan]) the efficiency is also reduced since  $\Delta V$  is increased.

Such design rules gained from simulations are very useful for the engineering of “novel” contacts. It helps to evaluate the actually limiting losses and finally the heterojunction parameters that need to be improved experimentally.

### 3 EXPERIMENTAL RESULTS

The limited validity and applicability of the diode equation for the loss analysis of contacts limited by an insufficient selectivity calls for a useful figure of merit for engineering such contacts towards sufficient selectivity. This is in contrast to selective contacts for which the “classical” electrical losses like recombination and ohmic transport are well quantified by  $J_0$  and the contact resistance. In this sense, we can determine  $\Delta V$  which is experimentally accessible without much effort for open-circuit conditions [12]. For further insight the

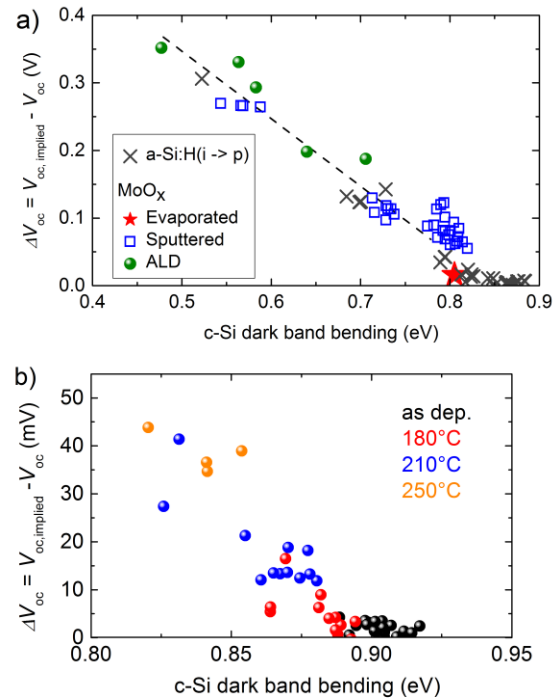


**Figure 5:**  $\Delta V_{\text{oc}}$  for different hole contacts as a function of the induced c-Si band bending. The latter is determined by surface photo-voltage (SPV) measurements. a) Influence of fabrication conditions for a-Si:H(p) and  $\text{MoO}_x$ . b) Influence of post deposition annealing for thermally evaporated  $\text{MoO}_x$ .

induced band bending can be measured by surface photo-voltage measurements or C-V.

For the sake of completeness, it shall be pointed out that a similar way to probe the selectivity is to take advantage of the fact that the selectivity is (further) decreased by increasing the illumination intensity above 1 sun. On the one hand, this increases the sensitivity for assessing a small  $\Delta V$  for 1 sun conditions which might be limited by the measurement accuracy. On the other hand the increase of  $\Delta V$  with illumination causes a characteristic slope of the Suns- $V_{\text{OC}}$  characteristic reflecting a very low or negative ideality factor of a corresponding diode equation [12], [13]. Such ideality factors lack physical meaning, substantiating the limited validity of the diode equation for non-selective contacts.

#### 3.1 Probing the selectivity

The importance of the induced c-Si junction for a low  $\Delta V_{\text{oc}}$  is shown in Figure 5a for different hole contacts: A doping variation for p-type a-Si:H [12] and  $\text{MoO}_x$  which

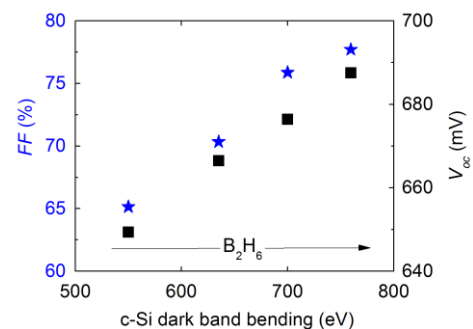


**Figure 6:** Influence of induced c-Si band bending for a-Si:H(p) emitter doping of silicon heterojunction cells.

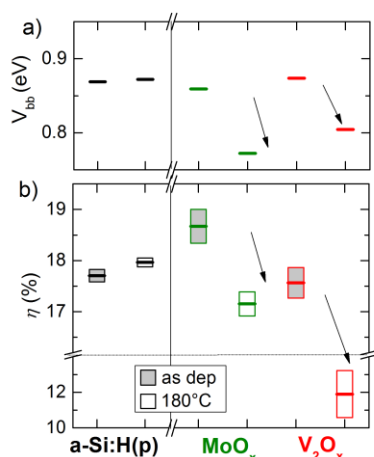


**Figure 7:** a) Induced c-Si band bending for test structures and b) efficiency of simple silicon heterojunction cells featuring different hole contacts before and after annealing.

is deposited by thermal evaporation [14], ALD [15] or sputtering [16]. Good qualitative agreement with the simulation results is obtained. Most important, a linear dependence of  $\Delta V_{oc}$  on the induced c-Si band bending is obtained. A higher band bending and lower  $\Delta V_{oc}$  results from higher doping of the p-type a-Si:H(p). For MoO<sub>x</sub> only thermal evaporation enables a high band bending and good selectivity. However, Figure 5b shows that a post deposition annealing has a negative influence on the band bending and  $\Delta V_{oc}$  for MoO<sub>x</sub> [17]. The loss of band bending suggests that a reduction of the effective work function of the MoO<sub>x</sub> is involved in the reduction of selectivity. This degradation of the selectivity highlights the main challenge for the application of MoO<sub>x</sub>, but also other currently investigated materials: The successful integration of such materials in the c-Si solar cell device architectures and the compatibility with the corresponding fabrication steps.

### 3.2 Proof of concept solar cells

The importance of the induced c-Si band bending for the silicon heterojunction featuring an a-Si:H(p) hole contact is shown in Figure 6. With increasing gas phase doping the band bending is increased resulting in improved  $FF$  and  $V_{oc}$ . That these improvements are caused by an improved selectivity is reflected in the disappearance of an s-shaped  $J-V$  characteristic, the temperature dependence of the  $V_{oc}$  and  $FF$ , the ideality factor obtained from Suns- $V_{OC}$  measurements and by the increased fulfilment of the superposition principle (overlap of dark and light  $J-V$  curve shifted by  $J_{sc}$ ) as shown in Ref. [18]. This is pointing towards the fact that “classical” losses and hence the validity of the diode equation becomes more dominant with increasing a-Si:H(p) doping.

The basic applicability of the two high work function transition metal oxides MoO<sub>x</sub> and V<sub>2</sub>O<sub>x</sub> for c-Si solar cells is shown in Figure 7b [19] and was explored by others [6], [20], [21]. Compared to the control device featuring an a-Si:H(p) hole contact encouraging efficiencies are obtained before annealing. However, annealing which is an integral part of the back-end cell processing results in a significant reduction of efficiency for MoO<sub>x</sub> and V<sub>2</sub>O<sub>x</sub> which is caused by the reduction of the selectivity as shown in Ref. [19]. It can be seen in

Figure 7a that this efficiency reduction comes along with a decrease of the induced c-Si band bending ( $V_{bb}$ ).

## 4 CONCLUSIONS

It was stressed that, in the un-optimized case, novel passivating and carrier selective contacts might not obey the diode theory which means that the “classical” electrical losses like recombination and ohmic transport which are well quantified by  $J_0$  and the contact resistance are not sufficient for contact evaluation. In such a case a useful figure of merit is needed for engineering the contact towards a sufficient selectivity and hence validity of the diode theory. In this sense, probing the voltage loss is suggested which occurs for non-selective contacts in the contact region during operation since low-injection conditions and an asymmetric majority / minority carrier conductivity are not maintained. A relatively simple experimental approach is to check if the external voltage matches the implied voltage during open-circuit conditions.

The need for a sufficient high induced c-Si band bending to obtain a selective contact was highlighted for a-Si:H(p) and two metal oxide based hole contacts.

## 5 ACKNOWLEDGEMENTS

K. Zimmerman and colleagues at ISE are gratefully acknowledged for experimental / technical assistance and fruitful discussions. This work was funded by the European project DISC under the European Union’s Horizon 2020 research and innovation program under grant agreement N°727529.

## REFERENCES

- [1] R. M. Swanson, "Approaching the 29% limit efficiency of silicon solar cells," in *Proceedings of the 31st IEEE Photovoltaic Specialists Conference*, Orlando, USA, 2005, pp. 889-94.
- [2] S. M. Sze, *Physics of semiconductor devices*, 2nd ed. New York: John Wiley & Sons, Inc., 1981.
- [3] P. Würfel, *Physics of Solar Cells - From principles to new concepts*. Weinheim: Wiley-Vch Verlag GmbH & Co KgaA, 2005.
- [4] F. Feldmann, *et al.*, "Passivated rear contacts for high-efficiency n-type Si solar cells providing high interface passivation quality and excellent transport characteristics," *Solar Energy Materials and Solar Cells*, vol. 120, pp. 270-274, 2014/01/01/ 2014.
- [5] R. Peibst, *et al.*, "Building blocks for back-junction back-contacted cells and modules with ion-implanted poly-Si junctions," in *2014 IEEE 40th Photovoltaic Specialist Conference (PVSC)*, 2014, pp. 0852-0856.
- [6] J. Geissbühler, *et al.*, "22.5% efficient silicon heterojunction solar cell with molybdenum oxide hole collector," *Applied Physics Letters*, vol. 107, p. 081601, 2015.
- [7] X. Yang, *et al.*, "High-Performance TiO<sub>2</sub>-Based Electron-Selective Contacts for Crystalline Silicon Solar Cells," *Advanced Materials*, pp. n/a-n/a, 2016.
- [8] J. Bullock, *et al.*, "Survey of dopant-free carrier-selective contacts for silicon solar cells," in *2016 IEEE 43rd Photovoltaic Specialists Conference (PVSC)*, 2016, pp. 0210-0214.

- [9] R. Singh, *et al.*, "Review of conductor-insulator-semiconductor (CIS) solar cells," *Solar Cells*, vol. 3, pp. 95-148, 1981.
- [10] L.-M. Chen, *et al.*, "Interface investigation and engineering - achieving high performance polymer photovoltaic devices," *Journal of Materials Chemistry*, vol. 20, pp. 2575-2598, 2010.
- [11] C. Messmer, *et al.*, "Numerical Simulation of Silicon Heterojunctions Featuring Metal Oxides," *Submitted to IEEE-JPV 2017*.
- [12] M. Bivour, *et al.*, "Doped Layer Optimization for Silicon Heterojunctions by Injection-Level Dependent Open-Circuit Voltage Measurements," *IEEE Journal of Photovoltaics*, pp. 566-574, 2014.
- [13] S. W. Glunz, *et al.*, "Analyzing back contacts of silicon solar cells by suns-voc-measurements at high illumination densities," in *Proceedings of the 22nd European Photovoltaic Solar Energy Conference* Milan, Italy, 2007, pp. 849-53.
- [14] M. Bivour, *et al.*, "Molybdenum and Tungsten Oxide: High Work Function Wide Band Gap Contact Materials for Hole Selective Contacts of Silicon Solar Cells," *Solar Energy Materials and Solar Cells*, pp. 34-41, 2015.
- [15] M. Bivour, *et al.*, "Atomic Layer Deposited Molybdenum Oxide for the Hole-selective Contact of Silicon Solar Cells," *Energy Procedia*, vol. 92, pp. 443-449, 2016/08/01/ 2016.
- [16] M. Bivour, *et al.*, "Sputter-deposited  $\text{WO}_x$  and  $\text{MoO}_x$  for hole selective contacts," *Energy Procedia*, 2017.
- [17] L. Neusel, *et al.*, "Selectivity issues of  $\text{MoO}_x$  based hole contacts," *Energy Procedia*, 2017.
- [18] M. Bivour, "Silicon Heterojunction Solar Cells: Analysis and Basic Understanding " PhD, Faculty of Engineering University of Freiburg, 2015.
- [19] M. Bivour, *et al.*, "High work function metal oxides for the hole contact of silicon solar Cells," in *2016 IEEE 43rd Photovoltaic Specialists Conference (PVSC)*, 2016, pp. 0215-0220.
- [20] L. G. Gerling, *et al.*, "Transition metal oxides as hole-selective contacts in silicon heterojunctions solar cells," *Solar Energy Materials and Solar Cells*, vol. 145, pp. 109-115, 2016.
- [21] M. Mews, *et al.*, "Oxygen vacancies in tungsten oxide and their influence on tungsten oxide/silicon heterojunction solar cells," *Solar Energy Materials and Solar Cells*, vol. 158, Part 1, pp. 77-83, 2016.